Boletim da Sociedade Astronômica Brasileira, **32**, no. 1, 31-35

Spot temperature from multiwavelength transit observations of CoRoT-2 b

A. O. Kovacs[1] & A. Valio[1]

[1] Universidade Presbiteriana Mackenzie, São Paulo, Brazil e-mail: andre.kovacs@mackenzista.com.br, avalio@craam.mackenzie.br

Abstract. Much like the Sun, measurements of radius and temperature of starspots in young solar-like stars are key parameters to quantify the level of magnetic activity in such stars. The magnetic activity can be particularly impactful in stars hosting transiting exoplanets, because it induces brightness variations that negatively impact the accuracy of exoplanet transit measurements. In particular, these variations can affect the transit depth estimates, having the potential to alter planetary transmission spectra, that could undermine the interpretation of results in exoplanet atmospheric characterizations. In this study, we employ the transit mapping method to probe starspot-crossing events of the solar-like star CoRoT-2, in transit observations of the exoplanet CoRoT-2 b, using archival observations from the CoRoT space mission, using its three colors (blue, green, and red) from the exoplanet channel. From the intensities of these spots, we estimate the temperatures assuming a blackbody emission and employing a PHOENIX stellar atmospheric model, as well as the relative sizes for the spots. Our results point to spots up to about 200 K cooler than the stellar photosphere (5529 K) and having radii of 0.31 stellar radii, or 196 Mm, and both larger than values from previous studies for CoRoT-2 in white light, corresponding to solar penumbra temperatures for spots much larger than typical sunspots. So, we can conclude that the degeneracy between the radius and the intensity of the spots, present in the analysis in "white light", can underestimate the size and intensity of the starspots.

Resumo. Assim como para o Sol, as medidas do radio e temperatura de manchas estelares em estrelas jovens similares ao Sol são parâmetros chave para quantificar o nível da atividade magnética em tais estrelas. A atividade magnética pode ser particularmente impactante em estrelas hospedeiras de exoplanetas em trânsito, por induzir variações de brilho que impactam negativamente a acurácia das medições de trânsitos dos exoplanetas. Em particular, tais variações podem afetar as estimativas da profundidade do trânsito, tendo o potencial de alterar os espectros de transmissão, que pode prejudicar a interpretação dos resultados em caracterizações atmosféricas dos exoplanetas. Neste estudo, amplicamos o método do mapeamento de trânsito para sondar eventos de cruzamento de manchas estelares da estrela CoRoT-2, semelhante ao Sol, por observações de trânsito do exoplaneta CoRoT-2 b, utilizando observações arquivadas da missão espacial CoRoT, fazendo o uso das suas três cores (azul, verde e vermelho) do canal de exoplanetas. A partir das intensidades das manchas, investigamos as temperaturas assumindo uma emissão de corpo negro e empregando um modelo atmosférico estelar PHOENIX, assim como os tamanhos relativos para as manchas. Nossos resultados apontam para manchas cerca de até 200 K mais frias do que a fotosfera estelar (5529 K) e tendo raio de 0,31 raios estelares, ou 196 Mm, com ambos valores maiores do que valores de estudos prévios para a CoRoT-2 em "luz branca", correspondendo à temperaturas da penumbra solar para manchas muito maiores do que as manchas solares típicas. Desta forma, podemos concluir que a degenerescência entre o raio e a intensidade das manchas, presente nas análises em "luz branca", pode subestimar o tamanho e a intensidade das manchas estelares.

Keywords. (Stars:) starspots – Stars: activity – Stars: planetary systems

1. Introduction

As known for the Sun, starspots have also been observed in stars like it, pointing to the existence of similar processes of magnetic activity. However, unlike the Sun, currently the identification of spots in other stars can only be done indirectly. Among the available observational techniques, the planetary transit mapping method is particularly favorable for modeling the presence of starspots in the stellar photosphere. It relies only light curves from photometric observations of exoplanets transiting their host star, using the residuals from the transit model fit Silva (2003). Currently, more than 6000 exoplanets are known, most of them transiting planets ($\sim 75\%$), which favors the use of the planetary transit mapping method.

Much like the Sun, CoRoT-2 is a G-type star, also magnectively active and having comparable mass and radius (0.97 $M_{\odot}$ e 0.902 $R_{\odot}$), but a little colder (5625 K) (Alonso et al. 2008). During the CoRoT (*Convection, Rotation, and Transit*) mission, the star CoRoT-2 had its brightness monitored uninterruptedly for approximately 5 months in 2007. The observations produced photometric data of unprecedented quality for the time and allowed the discovery of the exoplanet CoRoT-2 b, a gas giant that orbits its host star approximately each 1.7 terrestrial days. A total of 82 transits of the planet in front of its star were detected (Alonso et al. 2008).

However, given the magnetic activity of the host star, the light curves from the transit observations of CoRoT-2 b, much like in outside of transit and spectroscopic observations, display contamination mainly from the presence of starpots. These induce noise in the data that difficults the correct determination of the parameters of the fit of the exoplanet transit model. Besides that, differently from what is done in studies of solar magnetic activity, the impossibility of directly resolving characteristics on the stellar photosphere forces the use of indirect methods to infer the presence and attributes of spots on the stellar surface. Given its similarity to the Sun, the star CoRoT-2 became the reference target in studies of stellar activity characterization for main sequence stars.

Initially, the mapping of starspot distribution was performed for eclipsing binary stars. However, the contamination of the data from stellar activity became a major problem with the advent of photometric observations of transiting exoplanets by space mission like CoRoT and Kepler, and the low resolution

spectroscopy from space by the Hubble Space Telescope (HST) and James Webb Space Telescope (JWST). Due to the superior photometric precision of space telescopes over ground ones, the contamination from starspots enhanced its negative impact on studies of atmospheric characterization of exoplanets via transmission spectroscopy (Rackham, Apai, & Giampapa 2018). This is mainly because space observations are capable of achieving a higher level of photometric precision in relation to observations from the ground, and allow a better distinction of individual spots (Silva-Valio, Lanza, Alonso, & Barge 2010).

Thus, the increase in photometric precision provided by space telescopes such as NASA's JWST and the future ESA missions PLATO and ARIEL will make possible the study of exoplanets with sizes comparable to that of Earth. In these cases, contamination from starspots in transit observations will become more evident. This contamination affects the estimation of the planet's radius and orbital parameters and, consequently, influences the characterization of its atmosphere through the transmission spectroscopy technique.

Given these factors, the study of stellar activity is of utmost importance for future exoplanet observations, having the exoplanet CoRoT-2 b as an usual reference target in studies of stellar contamination from starspots, to comprehend and mitigate their interference on observations. The studies of stellar activity by Silva (2003) and Silva-Valio, Lanza, Alonso, & Barge (2010) for the star CoRoT-2, with the data from the CoRoT mission, were pioneers in modeling the contamination by occulted starspots in transits of exoplanets, with the so called planetary transit mapping method and the ECLIPSE tool. The tool adopts an approach of discrete circular spots to model the stellar contamination, using a representation according to a two-dimensional grid of high resolution that represents the stellar surface with spots, and the computation of transit model via numerical integration. Later, several other implementation variations have already been proposed in the literature (Béky, Kipping, & Holman 2014). The planetary transit mapping method offers advantages over the Doppler imaging method since, in principle, it allows the detection of small spots ($\sim$ 50 Mm) in the surface of Sun-like stars, during the transit of Earth-like planets (Lanza 2016).

From the observational point of view, much like in solar activity studies, two of the most important parameters in the caracterization of the stellar activity are the size and the temperature of the spots, since they allow to quantify the stellar magnetic activity. In particular, the spot temperature allows to estimate the age and measure magnetic activity cycles of the star, given that more intense magnetic fields produce cooler spots which are associated to the dynamo process, and to its evolutionary state (Berdyugina 2005). However, the correct determination of the starspots' properties by the planetary transit mapping method depends on observations in multiple photometric bands. This occurs because of the degeneracy between the radius and the intensity of the spots (Rosich et al. 2020), as well as the necessity of spot intensity measurements in multiple colors to correctly determine their temperature (Schutte et al. 2023).

Since spots' intensity are dependent of the observed color, observations in multiple photometric bands is more advantageous than monochromatic data. This work extends previous studies of the magnetic activity of CoRoT-2, which modeled the contamination in the transits of CoRoT-2 b Silva-Valio, Lanza, Alonso, & Barge (2010) using monochromatic CoRoT data and the ECLIPSE tool Silva (2003). We now apply this analysis to the three different color channels (blue, green, and red) of the CoRoT exoplanet detector, thereby improving the original method.

Specifically, we start by describing our approach for multi-band photometry with data from the CoRoT mission in Section˜2, followed by the models employed to represent the spot contaminated transit light curve. The computed blackbody and PHOENIX spectra are presented in Section 3, and the results for the fits of both types of models in Section˜4. Finally, we discuss our results in light of previous studies and list our conclusions in Section 5.

2. Multi-band photometry by the CoRoT mission

Previous studies of the stellar activity of CoRoT-2 with data from the CoRoT mission made use only of the light curve in "white light" (Lanza et al. 2009; Huber, Czesla, Wolter, & Schmitt 2009, 2010; Silva-Valio, Lanza, Alonso, & Barge 2010). These were obtained from the combination of the signals from the different individual chromatic channels, despite the chromatic information present in the distinct individual channels (red, green, and blue) of the exoplanet detector, which could provide a higher signal-to-noise ratio. This occurred, probably in part due to the challenges of modeling the spectral response for the individual channels generated by the low dispersion prism positioned in front of the detector (CCD) and the respective onboard parameters for the star, in addition to the lower computational effort required to fit only a single photometric band.

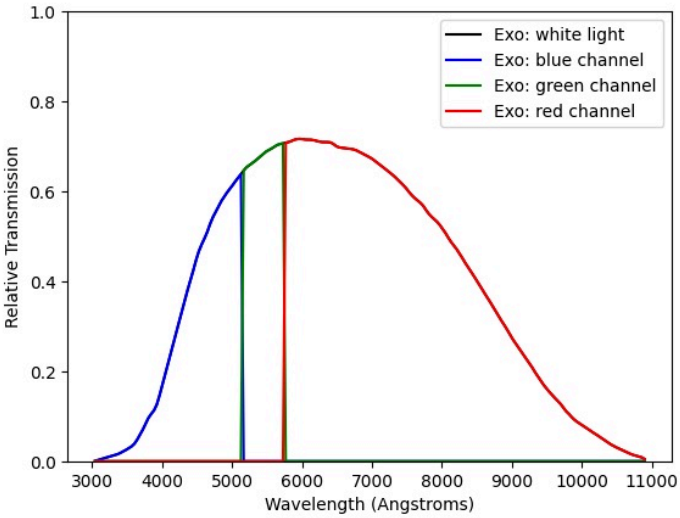

FIGURE 1: Response curves obtained for the three color channels (blue, green, and red) for the exoplanet observing instrument, from the "white light" response curve in Auvergne et al. (2009).

However, we identified that a procedure similar to that used by the CoRoT exoplanet instrument, where the point spread function (PSF) of the stellar image was separated into different color channels during photometric data reduction (Auvergne et al. 2009), can also be applied here. The response curve available for the "white light" data can be partitioned into three broad bands corresponding to the colors of the individual channels. This makes it possible to reproduce the intensity of each channel from the integrated white-light signal. Using this artifice, we could generate the response curves for the individual channels (see Figure 1), and we identified that it was possible to generate individual limb darkening coefficients for each of the color channels. Moreover, during our preliminary tests, we identified that the chromatic information present in each different spot intensities for each color channel was still detectable in the joint

chromatic fit of transit models of CoRoT-2 b with spots present on the transit chord, albeit a smaller signal-to-noise of the channels.

The exoplanet CoRoT-2 b was observed within the field of view denominated LRc01, during the period from May 9, 2007 to October 15, 2007, and its host star received initially the identifier CorotID 0101206560, until the confirmation of the transiting exoplanet, when the star began to be called CoRoT-2 and the exoplanet CoRoT-2 b (originally CoRoT-Exo-2b). The initial observations were conducted in a 512 s cadence, changing to a 32 s cadence as soon as the first detections of the exoplanet transit, to allow a higher quality for the transit analysis (Alonso et al. 2008). Thus, the data set provides the individual intensities for each color channel (blue, green, and red) and their corresponding error estimates, computed on board, as well as the combined intensity in the "white light", computed on the ground (Chaintreuil et al. 2016; Deleuil & Fridlund 2018).

3. Methods

Given that we consider here only three distinct wavelengths (λ), we adopted the representation of the starspots by the planetary transit mapping method in its non-parametric form, i.e., without assuming any restriction for the spot intensities by the model, considering the problem in its complete dimensionality. Thus, the parameters for the radii ($R_{spot,i}$), longitude ($long_{spot,i}$), and latitude ($lat_{spot,i}$) are common for each spot, for different λ, whereas the intensities per wavelength ($I_{spot,i,\lambda}$) are different. The latitude of the spots was assumed to be the same as the latitude of the transit chord, and fixed at $-23.7°$.

To estimate the relative fluxes of the starspots in each color channel, measured in $erg/s/cm^2$, from the fitted parameters for the contaminated transit of CoRoT-2 b, we scaled the stellar spectra at the particular wavelength by the intensity of the spots in each corresponding color. For this, we assumed both a blackbody curve and a PHOENIX spectrum for the photosphere of CoRoT-2 and an effective temperature for the star of $T_{eff} = 5529$ K (Stassun et al. 2019).

The blackbody curve adopts the Planck function for its fluxes, employing the package `Synthetic Photometry (synphot)`[1] (STScI Development Team 2018), whereas for the PHOENIX spectra we employed the package `Synthetic Photometry for HST (stsynphot)` [2] (STScI Development Team 2018). The same models were assumed later in the MCMC fits of the spot fluxes in each color channel wavelength, to estimate the temperature of each spot.

4. Results

To fit the signatures from the starspots on the planetary transit light curve, we used the level 2 (N2) data from the LRc01 run of the CoRoT mission in 2007, that are currently archived and publicly available on the CoRoT mission archive from IAS[3]. Using this data, and the Dynamic Nested Sampling algorithm implemented by the package `Ultranest`[4] (Buchner 2021), together with the planetary parameters from Alonso et al. (2008) and the stellar parameters from Chavero et al. (2010), we could validate the strategy of fitting simultaneously multiple contaminations of occulted starspots by the planetary transit in the chromatic light

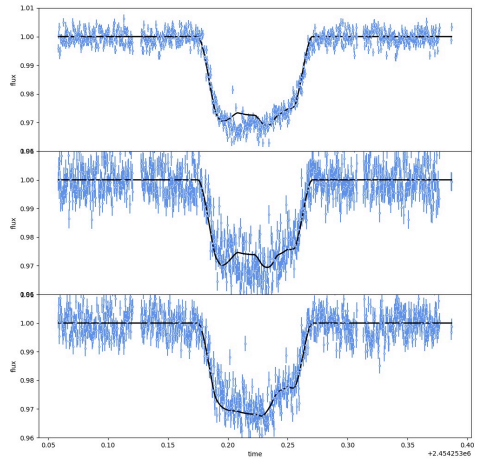

(a) Light curves

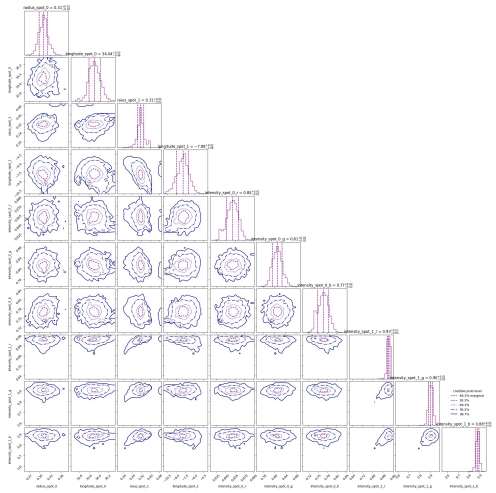

(b) Posterior distributions

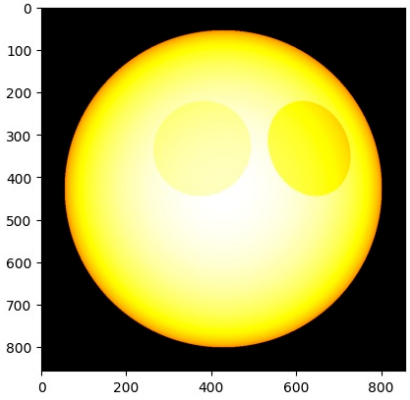

(c) Surface map

FIGURE 2: Results from the transit model fit of CoRoT-2 b in the photometric bands, for the transit centered on 2454253.22284 BJD, containing the contamination from two spots: a) The blue dots show the data from the light curves in the red, green, and blue colors on the top, center, and lower panels, in this order. b) Posterior distributions of the spot parameters used in the simultaenous fit of both spots in the three colors. c) Surface map containing the visual representation of the fitted spots on the stellar surface.

[1] `https://synphot.readthedocs.io/en/latest/`
[2] `https://stsynphot.readthedocs.io/en/latest/`
[3] `http://idoc-corot.ias.u-psud.fr/`
[4] `https://johannesbuchner.github.io/UltraNest/index.html`

	Color	R_{spot} (R_{star})	Intensity	longitude (°)
Spot 1	Red	$0.31^{+0.01}_{-0.01}$	$0.85^{+0.01}_{-0.01}$	$+34.0^{+0.5}_{-0.4}$
	Green	...	$0.81^{+0.02}_{-0.02}$	...
	Blue	...	$0.77^{+0.02}_{-0.02}$	...
Spot 2	Red	$0.31^{+0.09}_{-0.02}$	$0.93^{+0.01}_{-0.01}$	$-7.9^{+0.9}_{-1.1}$
	Green	...	$0.90^{+0.02}_{-0.02}$	...
	Blue	...	$0.88^{+0.01}_{-0.02}$	...

TABLE 1: Starspot parameters derived from the MCMC fit for the two detected spots. The table includes the spot radius in stellar radii (R_{spot}/R_{star}), intensity relative to the stellar disk center, and longitude (in degrees) for both spots per CoRoT color. The uncertainties reflect the range of possible values obtained through the MCMC analysis.

curves. As shown in Figure 2, the simultaneous fit in multiple colors breaks the degeneracy between the radius and intensity parameters for both identified spots. This approach yields well-defined Gaussian posteriors for these parameters. The result is achieved through a non-parametric strategy in which the latitude, longitude, and radius of the spots are shared across all three colors, while only the spot intensities are allowed to vary from one color to another.

As to the spots' temperature estimate, we fit the relative fluxes obtained for the spots in the respective 3 wavelengths, obtained following the procedure described above (see Section 3), using the blackbody and PHOENIX spectra, as shown in Figures 3 and 4. It is possible to verify that, as expected, both spots provided temperatures lower than the chromospheric temperature of the star CoRoT-2, with uncentainties lower than 10 K, attesting the high precision obtained for the spot fit parameters.

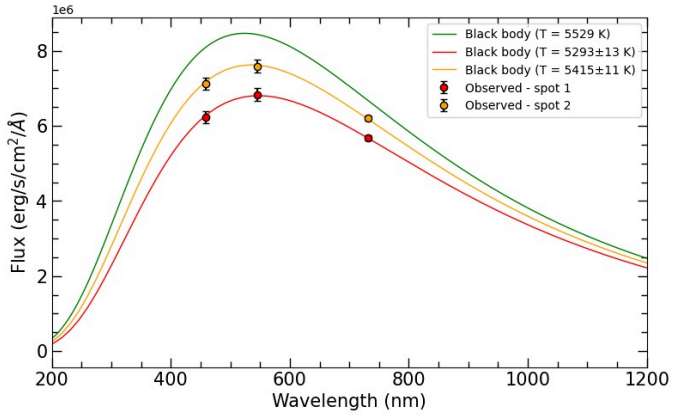

FIGURE 3: Starspot temperature estimation using the blackbody fitting. The red and orange dots represent the observed spot intensities in the three colors (red, green, and blue), whereas the red and orange curves correspond to the best-fit blackbody spectra, yielding temperatures of 5293 ± 13 K for the first spot (longitude of 34.0°) and 5415 ± 11 K for the second spot (longitude of −7.9°). The stellar photosphere is assumed to have an effective temperature of 5529 K (green curve).

The temperatures obtained from the fit of atmospheric models were 5293 ± 13 K for the first spot (longitude of 34.0°) and 5415 ± 11 K for the second spot (longitude of −7.9°) for the blackbody case (see Table 2 and Figure 3), and 5394 ± 5 K for the first spot (longitude of 34.0°) and 5418 ± 11 K for the second spot (longitude of −7.9°) for the PHOENIX case (see Table 3 and Figure 4), having both cases assumed a photospheric temperature of 5529 K.

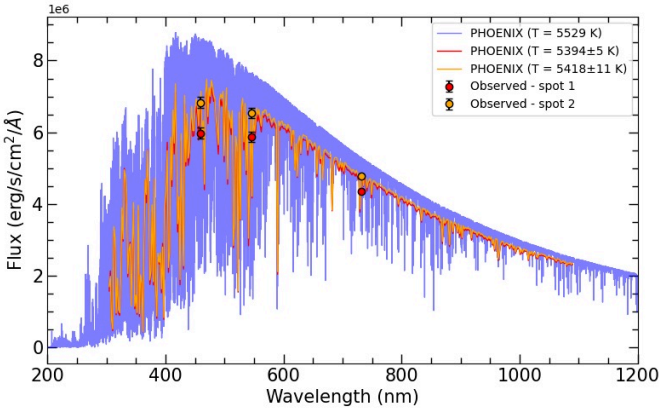

FIGURE 4: Starspot temperature estimation using the PHOENIX stellar atmosphere models. The red and orange points represent the observed spot intensities in the three colors (red, green, and blue), whereas the red and orange curves correspond to the best-fit PHOENIX spectra, yielding temperatures of 5394±5 K for the first spot (longitude of 34.0°) and 5418±11 K for the second spot (longitude of −7.9°). The stellar stellar photosphere is assumed as a PHOENIX spectrum for a 5529 K star, having log(g) = 4.48, [Fe/H] = -0.04, and [α/M] = 0.0 (blue curve).

Spot	Color	λ_{pivot} (nm)	Flux (10^6 erg/s/cm^2/Å)	Temperature (K)
1	Red	731.7	6.23±0.16	5293 ± 13
	Green	545.0	6.83±0.17	
	Blue	458.4	5.67±0.07	
2	Red	731.7	7.12±0.16	5415 ± 11
	Green	545.0	7.59±0.17	
	Blue	458.4	6.21±0.07	

TABLE 2: Starspot temperatures derived from the MCMC fit of a blackbody model for the two detected spots. The table includes the wavelength (λ_{pivot}) of the CoRoT color, spot flux, estimated spot temperature (K) for both spots. The uncertainties reflect the range of possible values obtained through the MCMC analysis.

Spot	Color	λ_{pivot} (nm)	Flux (10^6 erg/s/cm^2/Å)	Temperature (K)
1	Red	731.7	5.98±0.16	5394 ± 5
	Green	545.0	5.88±0.15	
	Blue	458.4	4.36±0.05	
2	Red	731.7	6.83±0.16	5418 ± 11
	Green	545.0	6.53±0.15	
	Blue	458.4	4.773±0.05	

TABLE 3: Starspot temperatures derived from the MCMC fit of a PHOENIX model for the two detected spots. The table includes the wavelength (λ_{pivot}) of the CoRoT color, spot flux, estimated spot temperature (K) for both spots. The uncertainties reflect the range of possible values obtained through the MCMC analysis.

5. Discussion and Conclusions

Here, we fitted the contaminations by two starspots present on the transit chord for the 10th transit of the exoplanet CoRoT-2 b, observed by the Exo instrument of the CoRoT mission in 2007, using the light curves in the three color channels provided by

the onboard instrumentation. In modeling starspot during planetary transits, a degeneracy is present between the radius and the intensity parameters for the case of a single photometric band, where a small, cooler spot can produce the same flux deficit as a larger, warmer spot. So, here we employed a non-parametric representation for the starspot intensities between the different color channels via the ECLIPSE model, to successfully break this degeneracy.

Our spots have radii of $1.78 \pm 0.06\ R_p$ ($0.31 \pm 0.01\ R_*$, or 196 Mm) and $1.78 \pm 0.17\ R_p$ ($0.31 \pm 0.03\ R_*$, or 196 Mm) for the first and second spots, respectively. These radii are larger than the average value of $0.46 \pm 0.11 R_p$, for the 369 spots estimated by Silva-Valio, Lanza, Alonso, & Barge (2010), which contains our transit observation for CoRoT-2 b.

Similarly, since the intensity parameter represents the relative intensity of the spot in relation to the stellar intensity, our spot intensities ranging from 0.77 to 0.85 and from 0.88 to 0.93 for the first and second spots, respectively, have lower constrast than the average value of 0.55 ± 0.13 found for the 369 spots by Silva-Valio, Lanza, Alonso, & Barge (2010). Regarding the temperature estimates for the starspots, we obtained here values higher than the range of 4340 and 5260 K reported by Silva-Valio, Lanza, Alonso, & Barge (2010), which assumed a blackbody model. Here, the temperatures obtained by fitting the backbody model were 5293 ± 13 K for the first spot (longitude of 34.0°) and 5415 ± 11 K for the second spot (longitude of −7.9°), and of 5394 ± 5 K for the first spot (longitude of 34.0°) and 5418 ± 11 K for the second spot (longitude of −7.9°) for the PHOENIX case. Both cases assumed the stellar photosphere as having an effective temperature of 5529 K.

As is usually the case for space based data in relation to ground-based observations, our results provided more precise estimates for the spot parameters (radius, intensities, and temperatures) than the results previously obtained from the simultaneous observation of CoRoT-2 b in four photometric bands with the SPARC4 instrument of the Observatório do Pico dos Dias (Valio et al. 2025). Besides that, comparatively to Valio et al. (2025), where the spot radii ranged between 0.34 to 0.61 R_p (or 38 - 69 Mm) and 0.61 to 0.77 for the spot intensities, when each individual spot fitted per passband, we see that our spots are also larger and much closer to the photospheric intensitity. Therefore, our temperature estimates are consequently hotter than the results with the SPARC4 instrument of 5110 ± 140 and 5040 ± 190 for the backbody model, and 5130 ± 120 K and 5060 ± 200 K for the PHOENIX spectra. Similar results were also obtained by Valio et al. (2025) for an alternative parametric multi-λ fit assuming intensities described by a backbody curve, and obtaining spot temperatures of 5280 ± 180 and 5220 ± 230 for each spot.

Both results can be explained by the strong degeneracies between the spot radius and intensity in contamination models that rely either on the "white light" CoRoT data Silva-Valio, Lanza, Alonso, & Barge (2010) or on fitting each passband independently, as in the SPARC4 analysis (Valio et al. 2025). Larger spots with higher temperatures (or intensities closer to that of the stellar photosphere) can produce the same level of transit contamination as smaller, cooler spots (or those with lower intensity than the photosphere). passband.

However, because starspots imprint different levels of contamination to the light curves in multiband photometry, by employing the light curve data in the three colors from the CoRoT mission, our non-parametric model was capable to break this degeneracy. Therefore, we show in this study that, when multiple photometric passbands are used simultaneously in the fit of the stellar contamination present in light curves from transiting exoplanets, it is possible to break the degeneracies between the radius and the intensities in the model, obtaining values closer to the true parameters for the starspots, and doing so, obtaining better estimates for the temperature of such spots.

Acknowledgements. A.O.K. acknowledges funding from CAPES. This study was financed in part by the Coordenação de Aperfeiçoamento de Pessoal de Nível Superior - Brasil (CAPES) - Finance Code 001. The authors thank the MackCloud (https://mackcloud.mackenzie.br), Multidisciplinary Laboratory of Scientific Computing and Cloud of the Universidade Presbiteriana Mackenzie, for the support in the execution of this research.

References

Alonso, R., Auvergne, M., Baglin, A., et al. 2008, A&A, 482, L21.
Auvergne, M., Bodin, P., Boisnard, L., et al. 2009, A&A, 506, 411.
Béky, B., Kipping, D. M., & Holman, M. J. 2014, MNRAS, 442, 3686.
Berdyugina, S. V. 2005, Living Reviews in Solar Physics, 2, 8.
Buchner, J. 2021, The Journal of Open Source Software, 6, 3001.
Chaintreuil, S., Deru, A., Baudin, F., et al. 2016, The CoRoT Legacy Book: The Adventure of the Ultra High Precision Photometry from Space, 61.
Chavero, C., de La Reza, R., Domingos, R. C., et al. 2010, A&A, 517, A40.
Deleuil, M., & Fridlund, M. 2018, Handbook of Exoplanets, 79.
Huber, K. F., Czesla, S., Wolter, U., & Schmitt, J. H. M. M. 2009, A&A, 508, 901.
Huber, K. F., Czesla, S., Wolter, U., & Schmitt, J. H. M. M. 2010, A&A, 514, A39.
Lanza, A. F., Pagano, I., Leto, G., et al. 2009, A&A, 493, 193.
Lanza, A. F. 2016, Lecture Notes in Physics, Berlin Springer Verlag, 914, 43.
Rackham, B. V., Apai, D., & Giampapa, M. S. 2018, ApJ, 853, 122.
Rosich, A., Herrero, E., Mallonn, M., et al. 2020, A&A, 641, A82.
Schutte, M. C., Hebb, L., Wisniewski, J. P., et al. 2023, AJ, 166, 92.
Silva, A. V. R. 2003, ApJ, 585, L147.
Silva-Valio, A., Lanza, A. F., Alonso, R., & Barge, P. 2010, A&A, 510, A25.
Stassun, K. G., Oelkers, R. J., Paegert, M., et al. 2019, AJ, 158, 138.
STScI Development Team 2018, Astrophysics Source Code Library, ascl:1811.001.
STScI Development Team 2020, Astrophysics Source Code Library, ascl:2010.003.
Valio, A., Martioli, E., Kovacs, A. O., et al. 2025, ApJ, 992, 174.